

Xiujuan ZHANG, Xiaosu YI, Yuanze XU

## Phase separation time/temperature dependence of some thermoplastics-modified thermosetting systems

© Higher Education Press and Springer-Verlag 2008

**Abstract** The phase separation processes of various thermoplastics-modified thermosetting systems which show upper critical solution temperature (UCST) or lower critical solution temperature (LCST) were studied with emphasis on the temperature dependency of the phase separation times. It was found that the phase separation time-temperature relationship follows the Arrhenius equation. The cure-induced phase separation activation energy  $E_a$  (ps) generated from the equation is independent of the method used to measure phase separation time. In our experimental ranges it is found that  $E_a$  (ps) is independent of the thermoplastic (TP) content, TP molecular weight and curing rate but it varies with the cure reaction kinetics and the chemical environments of the systems.

**Keywords** polymerization induced phase separation, thermosetting, thermoplastic, time and temperature dependence, Arrhenius equation

### 1 Introduction

The earlier approaches used in the synthesis of rubber-modified thermosetting resins to improve fracture toughness invariably result in significant drops in stiffness and glass transition temperature of the product. After the concept of cure-induced phase separation (CIPS) was proposed by Inoue et al. [1,2] in the 1980s, many experimental and theoretical investigations have been carried out on toughening highly crosslinked thermosets with high performance engineering thermoplastics such as

polyethersulfone (PES) [3] polysulfone (PSF) [4], poly(ether-ether ketone) (PEEK) [5] and polyether imide (PEI) [6]. Since the mechanical properties of the toughened materials are closely related to their final morphologies, the studies have focused on phase separation mechanisms [1,2,7] and morphology control [8–12].

To explain various morphologies generated during cure, thermodynamic analysis of the Flory-Huggins-Staverman (F-H-S) theory was employed. It describes the spinodal and bimodal decomposition lines [3,14–17] but it hardly relates the structural parameters and the time dependency. The solubility parameters and group contribution approaches constitute the first level of the relation for miscibility but not for reaction-induced phase separation yet. The cure processes of thermosetting systems are carried out in a certain time-temperature window and the morphology generated during cure also greatly depends on the cure path [18]. The morphology evolution may be analyzed qualitatively using the time dependent Ginzberg-Landau equation (TDGL) of phase separation dynamics [19] but it provides no clues about the temperature dependence of phase separation time. It is important to make experimental studies systematically on the phase separation time-temperature dependence during curing considering the variations of the material parameters in a broad time-temperature space [20].

The CIPS process can be observed *in situ* by different techniques – rheology [21–23], small angle light scattering (SALS) and turbidity [7]. Rheology observes certain abrupt mechanical changes upon phase separation while SALS and turbidity trace the change of the optical mismatch between TP and TS rich domains during phase separation. SALS is most widely used to characterize the evolution of domain size quantitatively in TP and TS blends [6,7,24]. The application of SALS is limited by the degree of optical mismatch between blend components and it is not adequate to trace the early stage of the phase separation process [20,25].

In this work, we observed the early stage of CIPS in some TP/TS systems with a modified optical microscope system [26] and compared the microscope method with

Translated from *Acta Polymerica Sinica*, 2007, 8: 725–730 [译自: 高分子学报]

Xiujuan ZHANG, Yuanze XU (✉)  
The Key Laboratory of Molecular Engineering of Polymers,  
Ministry of Education, Department of Macromolecular Science,  
Fudan University, Shanghai 200433, China  
E-mail: yuanzexu@fudan.edu.cn

Xiaosu YI  
Institute of Aeronautic Materials, Beijing 100095, China

the rheology and SALS approaches for the whole CIPS process. Our study focused on the common features of phase separation time-temperature dependence by considering the effects of TP molecular weight, TP content, cure rate, cure agent content and the cure reaction mechanism.

## 2 Experiments

### 2.1 Materials

The epoxy monomer was based on commercial grade DGEBA (diglycidyl ether of bisphenol A) with average epoxide equivalent of 185 (Wuxi Synthetic Resin Co., Jiangsu, China). The cyclic anhydride cure agent was methyl tetrahydrophthalic anhydride (MTHPA; HY 918, Ciba-Geigy) and the anhydride initiator was benzyl-dimethyl amine (BDMA, Sigma, USA). The aromatic cure agent 4, 4'-methylenedianiline (DDM) and 4, 4'-diaminodiphenyl sulfone (DDS) were provided by Shanghai Reagent Co. (Shanghai, China). The 4, 4'-bis-maleimidodiphenyl methane (BMI) was provided by Beijing Aeronautical Manufacturing Technology Research Institute and the chain extension agent *o,o'*-diallylbisphenol A (DBA) was provided by Sichuan Jiangyou Insulating Material Co. The thermoplastic hydroxyl terminated polyethersulfones (PES) with  $[\eta] = 0.36, 0.43$  and  $0.53$  dL/g were all supplied by Jilin University (China). Phenolphthalein poly (ether ether ketone) (PEK-C,  $[\eta] = 0.43$  dL/g) was developed in Xuzhou Vat Chemical Co Ltd. Polyetherimides (PEI, Ultem 1000) was provided by General Electric Co.

### 2.2 Sample preparation

The PEI modified epoxy mixtures were prepared via a two-step process. A 10% (*W/W*) solution of PEI was made by dissolving it in methylene dichloride. The resulting solution was then mixed with the epoxy monomer at room temperature. Most of the solvent in the mixture was vaporized in a circulation oven at room temperature and the residual solvent was removed in a hot vacuum oven for 24 h at 80°C. Subsequently, the cure agent was added at 135°C for DDS, 90°C for DDM and 60°C for MTHPA (with different initiator BDMA contents).

For PEK-C and PES-modified epoxy systems, TP was directly dissolved in the epoxy monomers at 140°C. The cure agent was added in the same way as for the PEI systems. In the TGDDM/DGEBA/DDS/PEK-C blends, the mass ratio of TGDDM to DGEBA is 3:2.

For the preparation of BMI/DBA/PEK-C blends, PEK-C was dissolved in DBA at 135°C. BMI was added after the mixtures had cooled to 120°C. The mixture with a BMI to DBA molar ratio of 1:0.87 was stirred continuously until a transparent blend was obtained.

The loading level of TP to thermosetting precursors (mixture of epoxy monomer and hardener) is counted by phr (part per hundred resin). The loading level of the cure agent is stoichiometrically balanced without denotation.

### 2.3 Measurements

#### TOM

To observe the initial stage of phase separation, a lab-made computerized transmission optical microscope (TOM) system equipped with inverted optical design, long focusing objective lens and controllable oven was designed which allows long term observation and data collection with a high resolution of 0.2  $\mu\text{m}$  in a wide working temperature range (RT to  $\sim 250^\circ\text{C}$ ). The system can assign the onset of phase separation for systems with low refractive index differences and small domain sizes of as low as 1  $\mu\text{m}$ . This was not succeeded by conventional TOM and SALS [26].

The samples for TOM observation were prepared by pressing the melt between two pieces of cover glass with a thickness of about 0.2 mm. The moment when the morphological structure appeared was defined as the phase separation time  $t_{\text{ps}}$ . The value of  $t_{\text{ps}}$  at any particular temperature is the average of five tests with observation errors of around  $\pm 3\%$  as measured in various TP-modified TS systems [20,22,25]. We find that the phase separation times detected with different resolution optical lens are the same within an accuracy of  $\pm 3\%$  as shown in Table 1. The fact that the  $t_{\text{ps}}$  values are independent of the magnification of the TOM proves that the onset of phase separation has been observed. If the initial domains were smaller than the resolution of the TOM system, one should see them earlier with higher magnification. The physical reason for limited initial domain size was explained as the nature of spinodal decomposition by Inoue [1,27]. The limited value of initial fluctuation wavelength becomes the periodic size of phase domains in the early stage of phase separation before domain growth driven by interfacial tension so that the early stage of the spinodal decomposition can be observed at similar  $t_{\text{ps}}$  using different TOM magnification.

**Table 1** The effect of OM resolution on  $t_{\text{ps}}$  of TGDDM/DGEBA/DDS/PEK-C 10 phr system

$T/^\circ\text{C}$	$t_{\text{ps}}/\text{s}$ (1500X)	$t_{\text{ps}}/\text{s}$ (1200X)	$t_{\text{ps}}/\text{s}$ (760X)	error/%
210	228	227	220	-1.3-2.2
200	328	321	320	-0.9-1.5
190	469	466	464	-0.4-0.6
180	610	608	602	-0.8-0.5

### Dynamic rheological measurements

The rheological experiments were performed with a rotational rheometer with disposable parallel plates (gap 1 mm and diameter 40 mm) (ARES of TA Instrument Co.). The multiple frequency dynamic time sweeps were conducted under isothermal conditions using the time-resolved rheometric technique [28]. The rheometric measurement conditions were collected at frequencies of 1, 2, 5, 10 and 20 rad/s with an initial strain of 5%. The strain can be automatically adjusted to maintain the torque response within the limit of the transducer.

Figure 1 shows the characteristic rheological profiles with the corresponding morphological TOM micrographs of TGDDM/DGEBA/DDS/PEK-C systems along curing. There are two critical transitions in the plots of  $\tan \delta$  at different frequencies. The curves cross at the time for phase separation  $t_{ps}$  and the time for chemical gelation  $t_{gel}$  where loss tangent becomes independent of frequency [29, 30]. We have discussed such critical gel behaviors more systematically in previous work [20,22].

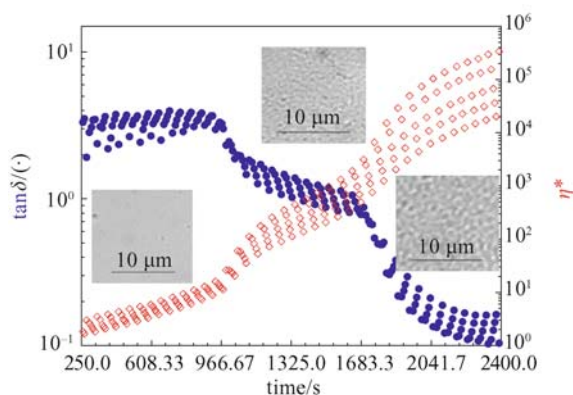


**Fig. 1** The  $\eta^*$  and  $\tan \delta$  versus time at different frequency cures and the corresponding morphology

### SALS

The phase separation time  $t_{ps}$  for some TP/TS blends with appropriate optical mismatch was also observed *in situ* by SALS using HeNe laser light ( $\lambda = 632.8$  nm). Samples were mounted in a temperature controllable hot-stage. The scattering pattern generated by the sample was visualized using a white paper screen and recorded by a standard CCD video camera. The time upon which the scattering ring appears is defined as the phase separation time.

### DSC

A differential scanning calorimetric analysis was conducted using a Perkin-Elmer Pyris 1 instrument. The calorimeter was calibrated with high purity indium and zinc standards. Dry nitrogen was used as purge gas with a flow

rate of 20 mL/min. The DSC curves scanned at different heating rates of 5, 10, 15, 20, 25°C/min allow the calculation of the activation energy of the overall curing reaction by the Kissinger method [31]:

$$E_a = -R * \frac{d \ln(\beta/T_p^2)}{dT_p^{-1}} \quad (1)$$

In the equation above  $\beta$  is the heating rate,  $T_p$  is the peak temperature,  $E_a$  is the cure activation energy and  $R$  is the gas constant.

## 3 Results and discussion

The phase separation time versus temperature data based either on rheology, TOM or SALS can be correlated by an equation of Arrhenius of the form [20,22,25]:

$$\ln t_{ps} = \ln k + \frac{E_a(ps)}{RT} \quad (2)$$

In the equation above,  $t_{ps}$  is the phase separation time,  $E_a(ps)$  is the phase separation activation energy,  $T$  is the absolute temperature and  $R$  is the universal gas constant.

### 3.1 Effect of the phase separation detection method

The CIPS process of LCST type DGEBA/MTHPA/PES systems was observed *in situ* using methods of SALS, TOM and rheology which detected the optical mismatch, morphological change and mechanical response of the material along cure, respectively. Actually, the SALS method observes heterogeneous structures with sizes above the micron level [7] while the present TOM approach has an optical resolution of 0.2  $\mu\text{m}$  and can concurrently give direct morphology evolution information. As shown in Fig. 2, the phase separation times  $t_{ps}$  based on different observations show an order: TOM first,

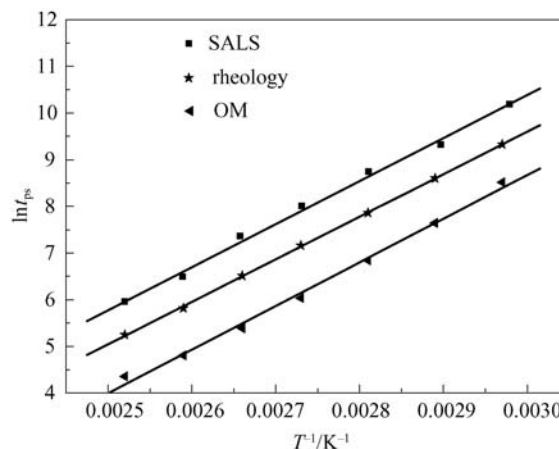


**Fig. 2** The effect of detecting method on  $E_a(ps)$  for DGEBA/MTHPA/PES system

then rheology and finally, SALS.  $E_a$ (ps) values are similar and are independent of observation method as seen in Table 2. In fact, we found that the phase separation time-temperature data in the literature also followed the Arrhenius equation as seen in the study of Pascault based on turbidity of castor oil modified epoxy system [32] and in that of Inoue based on light scattering of epoxy/dicyanamide/PES systems [33].

**Table 2**  $E_a$ (ps) values of DGEBA/MTHPA/PES system detected by different methods

detecting means	$E_a$ (ps)/kJ·mol <sup>-1</sup>	R
OM	77.8	0.997
rheology	75.8	0.999
SALS	76.7	0.999

### 3.2 Effect of TP content on $E_a$ (ps)

Figure 3 are the experimental data of  $\ln t_{ps}$  vs.  $1/T$  based on TOM measurements for the LCST type system DGEBA/MTHPA/PES [3] and UCST type system DGEBA/DDM/PEI [17] with different TP contents,

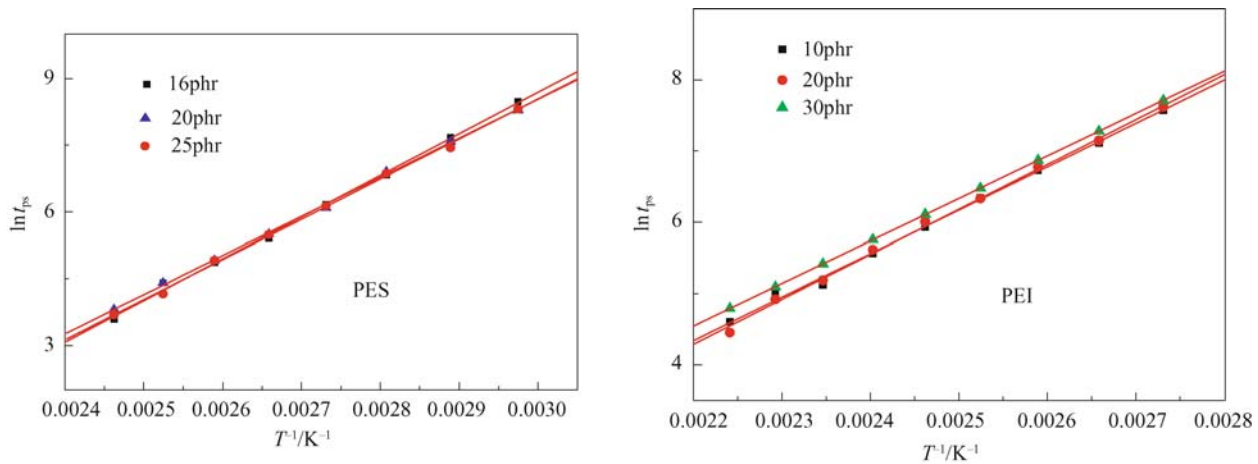


**Fig. 3** Effect of TP contents on the phase separation time/temperature dependence of DGEBA/MTHPA/PES and DGEBA/DDM/PEI systems

**Table 3**  $E_a$  (ps) values for DGEBA/MTHPA/PES and DGEBA/DDM/PEI systems with different TP contents

DGEBA/MTHPA/PES				DGEBA/DDM/PEI			
PES content/phr	$E_a$ (ps)/kJ·mol <sup>-1</sup>	R	$E_a$ /kJ·mol <sup>-1</sup>	PEI content/phr	$E_a$ (ps)/kJ·mol <sup>-1</sup>	R	$E_a$ /kJ·mol <sup>-1</sup>
16	77.8	0.999	70.7	10	50.6	0.999	51.6
20	73.0	0.999	/	15	52.4	0.999	/
25	75.0	0.999	70.4	30	49.5	0.999	52.3

**Table 4** Activation Energy Values of Phase Separation and Gelation for TGDDM/DGEBA/DDS/PEK-C Systems with different PEK-C contents

PEK-C content/phr	$E_a$ (ps, TOM)/kJ·mol <sup>-1</sup>	R	$E_a$ (ps, rheology)/kJ·mol <sup>-1</sup>	R	$E_a$ (gel, rheology)/kJ·mol <sup>-1</sup>	R
10	59.8	0.999	62.1	0.999	67.2	0.997
15	60.0	0.999	55.8	0.999	66.4	0.999
20	57.5	0.998	61.2	0.999	67.2	0.999

respectively. The corresponding phase separation activation energy  $E_a$  (ps) derived from the slope of the  $\ln t_{ps}$  vs.  $1/T$  plots is summarized in Table 3.

It can be found in Fig. 3 that for the two systems of DGEBA/MTHPA/PES and DGEBA/DDM/PEI with different TP contents,  $t_{ps}$  data in a wide temperature range can be correlated using the Arrhenius equation. The values of  $E_a$  (ps) in Table 3 are not sensitive to the TP content within the experimental range.

The driving force for the CIPS is the interaction change due to the cure reaction of the thermosetting species, so it is reasonable to correlate the cure reaction activation energy  $E_a$  to  $E_a$  (ps). The calculated  $E_a$  values are also listed in Table 3. It can be seen that the cure reaction energy barrier for systems with different TP contents is unchanged.

Table 4 are the phase separation time-temperature correlation results for a complex matrix resin system of TGDDM/DGEBA/DDS/PEK-C. Similar results can be seen for systems of TGDDM/DGEBA/DDS/PEK-C with different PEK-C contents. Similar  $E_a$  (ps, TOM) values are presented with reasonable accuracy. The phase

separation activation energy based on rheology,  $E_a$  (ps, rheology), is slightly higher than that based on TOM,  $E_a$  (ps, TOM). This is presumably due to the slight curing during rheology data collection at higher temperatures. It took about 2 minutes after sample loading for the plate temperature to stabilize. As we will see later in other systems the values of  $E_a$  (ps) based on different detection means are in good agreement.

It should be mentioned that the cure activation energy  $E_a$  may increase for high loading level of TP as reported by Park [34] and Francis [35] in other systems. Also, in our experiments the morphology does change from island to bi-continuous or phase inverted structure in the TP composition range of 5–30 phr, and the rheology profiles also change correspondingly although  $E_a$  (ps) hardly changes with the PEK-C content [20].

### 3.3 Effect of TP molar mass

Figure 4 is the phase separation time-temperature Arrhenius plot of DGEBA/MTHPA/PES systems with different PES molar mass. The corresponding  $E_a$ (ps) values are listed in Table 5. Bucknall [3] has determined cloud point curves of PES/DGEBA blends with PES of different molar mass and found that the miscibility will decrease with PES molar mass. Morphology will also change with the TP molar mass [36] but all these factors seem to have no effect on the values of  $E_a$ (ps).

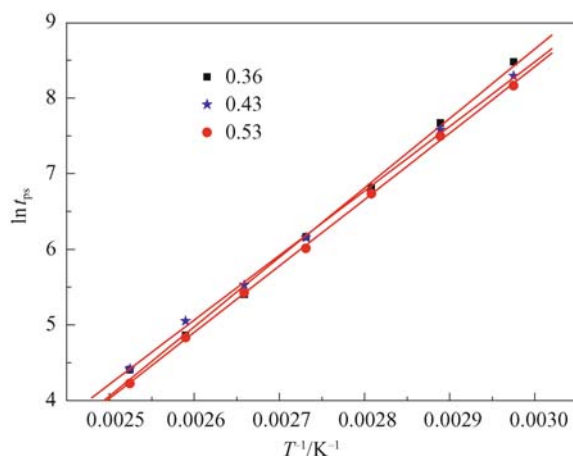


**Fig. 4** Effect of PES molar mass on the phase separation time-temperature dependence of DGEBA/MTHPA/PES systems

**Table 5**  $E_a$  (ps) values for DGEBA/MTHPA/PES system with different PES molar mass

$[\eta]/\text{dL}\cdot\text{g}^{-1}$	$E_a(\text{ps})/\text{kJ}\cdot\text{mol}^{-1}$	$R$
0.36	77.8	0.998
0.43	72.0	0.999
0.53	73.5	0.999

### 3.4 Effect of cure rate

Figure 5 are curves of  $\ln t_{ps}$  vs.  $1/T$  for DGEBA/MTHPA/PES systems with different initiator contents. The corresponding phase separation activation  $E_a$  (ps) values are given in Table 6. It can be seen that the phase separation times decrease with initiator content while  $E_a$ (ps) in Table 6 remains almost constant although the morphology changes with initiator content [37, 38].

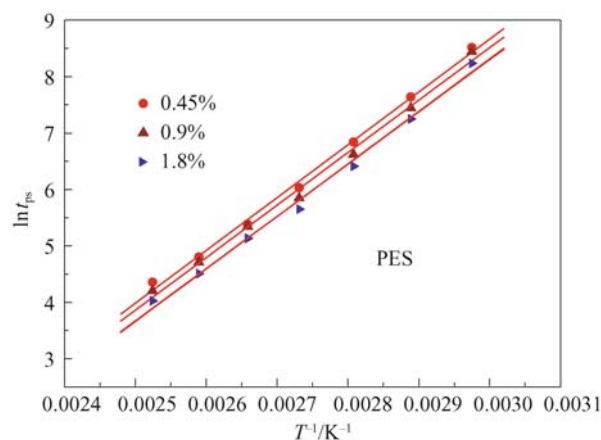


**Fig. 5** Effect of BDMA content on the phase separation time/temperature dependence for DGEBA/MTHPA/PES systems

**Table 6**  $E_a$  (ps) values for DGEBA/MTHPA/PES systems with different BDMA contents

BDMA content/%	DGEBA/MTHPA/PES		DGEBA/MTHPA	
	$E_a(\text{ps})/\text{kJ}\cdot\text{mol}^{-1}$	$R$	$E_a/\text{kJ}\cdot\text{mol}^{-1}$	$R$
0.45	77.8	0.998	73.9	0.999
0.9	77.8	0.999	73.8	0.999
1.8	77.0	0.99	73.9	0.999

We determined the cure activation energy  $E_a$  of the matrix resins with different BDMA contents. It can be seen in Table 6 that  $E_a$  is same for the systems with different BDMA contents. This is different from what Montserrat et al. [39] reported that the cure activation energy generally decreased with the initiator content. It is presumably because the initiator content employed in our present systems is high enough to catalyze the chain-wise copolymerization of DGEBA and MTHPA during the temperature scan. The high  $E_a$  values in Montserrat's systems arise from the uncatalyzed copolymerization when the initiator BDMA content is low.

When the initiator content is less than 2%, the chemical environment of the TP/TS blend will not change much with variation of BDMA concentration. It is interesting that even when the cure reaction driving force and chemical environment are similar, systems with different cure rates show similar  $E_a$  (ps) values.

### 3.5 Effect of stoichiometric ratio

The stoichiometric ratio of the system,  $r$ , is defined here as the molar ratio of anhydride groups to epoxy groups. It is reported that for some TP/TS blends, the morphology and mechanical properties of the cure TP/TS composites change substantially upon the variation of the stoichiometric ratio [40,41]. Here we report the data of DGEBA/MTHPA/PES 16phr systems with different  $r$  values. The experimental results are summarized in Fig. 6 and Table 7. It is understandable that the phase separation times of the system with  $r = 1.5$  are generally shorter than those of the systems with  $r = 0.5$  and  $r = 1.0$ . However, the corresponding activation energy  $E_a$  (ps) changes in an opposite manner with the stoichiometric ratio  $r$  as shown in Table 6.

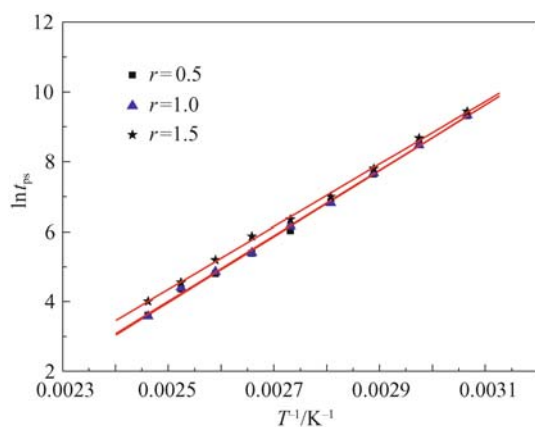


**Fig. 6** Plots of  $\ln t_{ps}$  vs.  $1/T$  for DGEBA/MTHPA/PES and systems with different stoichiometric ratio  $r$

**Table 7** Values of  $E_a$  (ps) for DGEBA/MTHPA/PES with different stoichiometric ratio  $R$

$r$	DGEBA/MTHPA/PES			
	$E_a(\text{ps})/\text{kJ}\cdot\text{mol}^{-1}$	$R$	$E_a/\text{kJ}\cdot\text{mol}^{-1}$	$R$
0.5	78.3	0.999	70.7	0.999
1.0	77.8	0.999	70.3	0.999
1.5	72.8	0.999	70.2	0.999

We first calculated the cure activation energy  $E_a$  for systems of different  $r$  value, and the results are similar as shown in Table 7. We know that for the CIPS process, in addition to the effect of entropy reduction, another important factor to the mixing free energy is the enthalpy contribution, which can be described qualitatively by the miscibility of the TP and TS components. It is expected that the less miscible the TP and TS combination are, the lower the phase separation activation energy  $E_a$  (ps). In our present systems, the TP/TS blends with different  $r$  values show similar cure reaction barrier. Thus, the decrease of  $E_a$  (ps) with excess MTHPA hardener can be attributed to the deterioration of the miscibility between TP and TS species by the hardener.

In the UCST systems of DGEBA/DDM/PEI and DGEBA/DDS/PEI [20] we observed similar phenomena, that is,  $E_a(\text{ps})$  changes with different affinities of TP/TS/Hardeners (Fig. 7). As shown in Table 8 the phase separation activation energy  $E_a(\text{ps})$  values of DGEBA/DDM/PEI and DGEBA/DDS/PEI systems change with  $r$  in different directions.

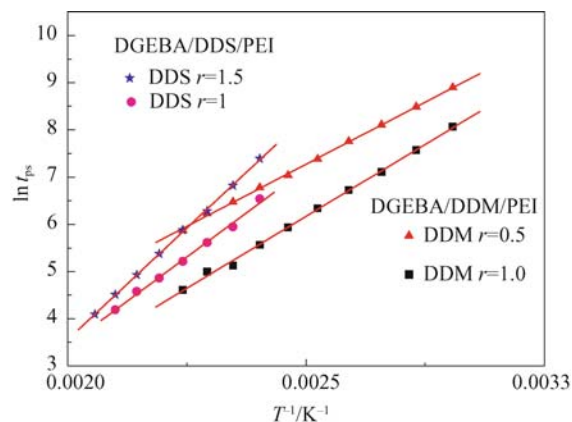


**Fig. 7** Linear correlations of  $\ln t_{ps}$  vs.  $1/T$  for the DGEBA/DDM/PEI and DGEBA/DDS/PEI systems with different  $r$

For DGEBA/DDM/PEI systems  $E_a$  (ps) increases with  $r$ , and the system even shows no phase separation when  $r = 1.5$ . For the DGEBA/DDS/PEI system,  $E_a$  (ps) changes with  $r$  in an opposite way to that of the DGEBA/DDM/PEI system.  $E_a$  does not change with the stoichiometric ratio  $r$  for both of the DGEBA/DDM/PEI and DGEBA/DDS/PEI systems. This is in accordance with the results of Yu et al. [41] for TGDDM/DDS systems that  $E_a$  changes little with  $r$  when  $r \geq 0.6$ . Therefore, the possible explanation of the change of  $E_a$  (ps) with  $r$  is not in the cure reaction but in the increased miscibility with PEI than DGEBA. The excess DDM stops phase separation upon cure. When the more polar DDS cure agent, which is less miscible with PEI than DGEBA, is used, the corresponding  $E_a$  (ps) changes with  $r$  in a different way.

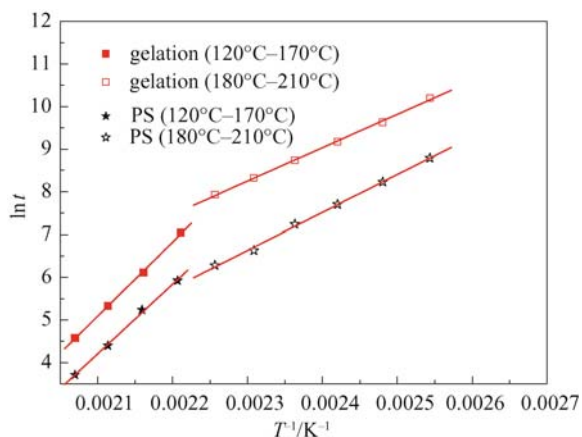
### 3.6 Effect of cure reaction

Figure 8 and Table 9 are the phase separation time-temperature relation in the range  $120^\circ\text{C}$ – $200^\circ\text{C}$  for system of BMI/DBA/PEK-C10 phr together with the gel time-temperature data. It can be seen that the slope of the phase separation time-temperature Arrhenius linear relation in the  $120^\circ\text{C}$ – $170^\circ\text{C}$  range is lower than that in the  $180^\circ\text{C}$ – $200^\circ\text{C}$  range. The phase separation activation energy  $E_a$  (ps) in Table 9 is smaller in the lower temperature range.

The change of temperature dependence of the phase separation times can be attributed to the complexity of the cure reaction between BMI and DBA. Although numerous attempts have been made to elucidate the curing

**Table 8** Values of  $E_a$  (ps) for the DGEBA/DDM/PEI and DGEBA/DDS/PEI systems with different  $r$ 

$r$	DGEBA/DDM/PEI		DGEBA/DDS/PEI	
	$E_a(\text{ps})/\text{kJ}\cdot\text{mol}^{-1}$	$E_a(\text{gel})/\text{kJ}\cdot\text{mol}^{-1}$	$E_a(\text{ps})/\text{kJ}\cdot\text{mol}^{-1}$	$E_a(\text{gel})/\text{kJ}\cdot\text{mol}^{-1}$
0.5	43.8	46.3	no ps	61.1
1.0	50.6	44.6	78.6	58.1
1.5	No ps	44.7	62.2	59.7

**Fig. 8** The phase separation time/temperature of BMI/DBA/PEK-C10phr system (by OM)**Table 9** Phase separation  $E_a$  of BMI/DABPA/PEK-C 10 phr system

$T/^\circ\text{C}$	BMI/DBA/PEK-C		BMI/DBA	
	$E_a(\text{ps})/\text{kJ}\cdot\text{mol}^{-1}$	$R$	$E_a(\text{gel})/\text{kJ}\cdot\text{mol}^{-1}$	$R$
120–170	73.7	0.999	54.3	0.999
180–200	136.0	0.999	120.3	0.999

mechanism of BMI/DBA systems, these have been impeded by the complexities of the reaction paths and multiple reactions taking place. The following reaction types have been proposed to be involved in the curing process: ENE, Diels–Alder, homopolymerization and alternating copolymerization. Allylphenol compounds are expected to coreact with BMI to give linear chain extension by an ENE-type reaction in the lower temperature range of 120°C–170°C and show a lower cure activation energy barrier. This is followed by a Diels–Alder reaction at the high temperature range of 180°C–200°C [42–46] with higher cure activation energy. It is probable that lower cure reaction energy barrier results in the low  $E_a$  (ps).

#### 4 Conclusions

The cure-induced phase separation time-temperature dependence can be described well using the Arrhenius equation. This has been verified in various TP modified TS systems. The phase separation times detected by different observation means such as TOM, rheology, SALS

and turbidity show different values at different stages but they all follow the Arrhenius equation with similar activation energy. Among the observation approaches, TOM is the fastest and most convenient means for determining the start of phase separation.

We know that most of the cure kinetics show Arrhenius type temperature dependence while the WLF type equation is also used for the process where macromolecular chain diffusion dominates the kinetics [47]. For our present cases, the cure induced phase separation also shows an Arrhenius type temperature dependency. This presumably arises from the strong asymmetric dynamic characteristics of the TP and TS species. The phase separation process mainly lies on the thermal diffusion of smaller TS species while the long chain TP component is pushed to a certain distribution. So  $E_a$  (ps) is not affected by the TP content and the TP molar mass and also has no relation to the cure rate but depends greatly on the diffusion ability of the TS species, the miscibility between TP and TS and the cure reaction energy barrier. More detailed analysis on the time-temperature dependency of the cure induced phase separation is underway [48].

#### References

- Inoue T. Reaction-induced phase-decomposition in polymer blends. *Progress in Polymer Science*, 1995, 20(1): 119–153
- Williams R J J, Rozenberg B A, Pascault J P. Reaction-induced phase separation in modified thermosetting polymers. *Polymer Analysis-Polymer Physics*, 1997, 128: 95–156
- Bucknall C B, Gomez C M, Quintard I. Phase-separation from solutions of poly(ether sulfone) in epoxy-resins. *Polymer*, 1994, 35(2): 353–359
- Min B G, Stachurski Z H, Hodgkin J H. Microstructural effects and the toughening of thermoplastic modified epoxy-resins. *Journal of Applied Polymer Science*, 1993, 50(9): 1511–1518
- Francis B, Rao V L, Jose S, Catherine B K, Ramaswamy R, Jose J, Thomas S. Poly(ether ether ketone) with pendent methyl groups as a toughening agent for amine cured DGEBA epoxy resin. *Journal of Materials Science*, 2006, 41(17): 5467–5479
- Bucknall C B, Gilbert A H. Toughening tetrafunctional epoxy resins using polyetherimide. *Polymer*, 1989, 30(2): 213–217
- Girard-Reydet E, Sautereau H, Pascault JP, Keates P, Navard P, Thollet G, Vigier G. Reaction-induced phase separation mechanisms in modified thermosets. *Polymer*, 1998, 39(11): 2269–2279
- Oyanguren P A, Aizpurua B, Galante M J, Riccardi C C, Cortazar O D, Mondragon I. Design of the ultimate behavior of tetrafunctional epoxies modified with polysulfone by

- controlling microstructure development. *Journal of Polymer Science Part B-Polymer Physics*, 1999, 37(19): 2711–2725
9. Brown J M, Srinivasan S, Rau A, Ward T C, McGrath J E, Loos A C, Hood D, Kranbeuhl D E. Production of controlled networks and morphologies in toughened thermosetting resins using real-time, in situ cure monitoring. *Polymer*, 1996, 37(9): 1691–1696
  10. Qian J Y, Pearson R A, Dimonie V L, Shaffer O L, El-Aasser, S. M. The role of dispersed phase morphology on toughening of epoxies. *Polymer*, 1997, 38(1): 21–30
  11. Mimura K, Ito H, Fujioka H. Improvement of thermal and mechanical properties by control of morphologies in PES-modified epoxy resins. *Polymer*, 2000, 41(12): 4451–4459
  12. Kim H R, Myung B Y, Yoon T H, Song K H. Enhanced fracture toughness of epoxy resins with novel amine-terminated poly (arylene ether sulfone)-carboxylic-terminated butadiene-acrylonitrile-poly (arylene ether sulfone) triblock copolymers. *Journal of Applied Polymer Science*, 2002, 84(8): 1556–1565
  13. Bucknall C B, Partridge I K. Phase-separation in cross-linked resins containing polymeric modifiers. *Polymer Engineering and Science*, 1986, 26(1): 54–62
  14. Verchere D, Sautereau H, Pascault J P, Moschiar S M, Riccardi C C, Williams R J J. Miscibility of epoxy monomers with carboxyl-terminated butadiene acrylonitrile random copolymers. *Polymer*, 1989, 30(1): 107–115
  15. Riccardi C C, Borrajo J, Williams R J J. Thermodynamic analysis of phase-separation in rubber-modified thermosetting polymers - influence of the reactive polymer polydispersity. *Polymer*, 1994, 35(25): 5541–5550
  16. Riccardi C C, Borrajo J, Williams R J J, Girard-Reydet E, Sautereau H, Pascault J P. Thermodynamic analysis of the phase separation in polyetherimide-modified epoxies. *Journal of Polymer Science Part B-Polymer Physics*, 1996, 34(2): 349–356
  17. Bonnaud L, Bonnet A, Pascault J P, Sautereau H, Riccardi C C. Different parameters controlling the initial solubility of two thermoplastics in epoxy reactive solvents. *Journal of Applied Polymer Science*, 2002, 83(6): 1385–1396
  18. Grillet A C, Galy J, Pascault J P. Influence of a 2-step process and of different cure schedules on the generated morphology of a rubber-modified epoxy system based on aromatic diamines. *Polymer*, 1992, 33(1): 34–43
  19. Tanaka, H. Viscoelastic model of phase separation. *Physical Review E*. 1997, 56(4): 4451–4462
  20. Zhang X J, Yi X S, Xu Y Z. Cure induced phase separation of epoxy/DDS/PEK-C composites and its temperature dependency. *Journal of applied polymer science*, 2007, accepted
  21. Xu J J, Holst M, Rullmann M, Wenzel M, Alig I. Reaction-induced phase separation in a polysulfone-modified epoxy-anhydride thermoset. *Journal of Macromolecular Science Part B-Physics*, 2007, 46(1): 155–181
  22. Zhang X J, Yi X S, Xu Y Z. Rheology and morphology development during phase separation and gelation of phenolphthalein polyether Eton modified epoxy resins. 22nd Annual Meeting of the Polymer Processing Society. Yamagata, Japan: Polymer Processing Society, 2006
  23. Bonnet A, Pascault J P, Sautereau H, Camberlin Y. Epoxy-diamine thermoset/thermoplastic blends. 2. Rheological behavior before and after phase separation. *Macromolecules*, 1999, 32(25): 8524–8530
  24. Gan W J, Yu Y F, Wang M H, Tao Q S, Li S J. Viscoelastic effects on the phase separation in thermoplastics-modified epoxy resin. *Macromolecules*, 2003, 36(20): 7746–7751
  25. Zhang X J, Xu Y Z. The rheological and morphological study of the phase separation and gelation process of TP modified TS systems. In: *Advances in rheology*. Jinan shandaong Shangdong University Press, 2006, 138–144 (in Chinese)
  26. Xu Y Z, Zhang X J. Inversed polarized hotstage microscope with high resolution, long working distance and high temperature duration. Chinese patent. 2007200666499
  27. Ohnaga T, Chen W J, Inoue T. Structure development by reaction-induced phase-separation in polymer mixtures - computer-simulation of the spinodal decomposition under the non-isoquench depth. *Polymer*, 1994, 35(17): 3774–3781
  28. Mours M, Winter H H. Time-Resolved Rheometry. *Rheologica Acta*, 1994, 33(5): 385–397
  29. Chambon F, Petrovic S Z, Macknight J W, Winter H H. Rheology of model polyurethanes at the gel point. *Macromolecules*, 1986, 19(8): 2146–2149
  30. Hess W, Vilgis A T, Winter H H. Dynamical critical-behavior during chemical gelation and vulcanization. *Macromolecules*, 1988, 21(8): 2536–2542
  31. Kissinger H E. Reaction kinetics in differential thermal analysis. *Analytical Chemistry*. 1957, 29(11): 1702–1706
  32. Chen D, Pascault J P, Sautereau H, Vigier G. Rubber-Modified Epoxies. 2. A reaction-induced phase-separation observed in-situ and a posteriori with different methods. *Polymer International*, 1993, 32(4): 369–379
  33. Kim, B S, Chiba T, Inoue T. A new time-temperature transformation cure diagram for thermoset thermoplastic blend - tetrafunctional epoxy poly(ether sulfone). *Polymer*, 1993, 34(13): 2809–2815
  34. Park S J, Kim H C, Lee J R. Studies on cure kinetics and rheological properties of difunctional epoxy/polysulfone blend system. *Polymer-Korea*, 2001, 25(2): 177–185
  35. Francis B, Poel G V, Posada F, Groeninckx G, Rao V L, Ramaswamy R, Thomas S. Cure kinetics and morphology of blends of epoxy resin with poly (ether ether ketone) containing pendant tertiary butyl groups. *Polymer*, 2003, 44(13): 3687–3699
  36. Yu Y F, Cui J, Chen W J, Li S J. Studies on the phase separation of polyetherimide modified tetrafunctional epoxy resin. II. Effects of the molecular weight. *Journal of Macromolecular Science-Pure and Applied Chemistry*, 1998, 35(1): 121–135
  37. Teng K C, Chang F C. Single-phase and multiple-phase thermoplastic thermoset polyblends. 1. kinetics and mechanisms of phenoxy epoxy blends. *Polymer*, 1993, 34(20): 4291–4299
  38. Cui J, Chen W J, Zhang Z C, Li S J. Studies on the phase separation of polyetherimide-modified epoxy resin. I. Effect of curing rate on the phase structure. *Macromolecular Chemistry and Physics*, 1997, 198(6): 1865–1872
  39. Montserrat S, Flaque C, Calafell M, Andreu G., Malek J. Influence of the accelerator concentration on the curing reaction of an epoxy-anhydride system. *Thermochimica Acta*, 1995, 269: 213–229
  40. Andres M A, Garmendia I, Valea A, Eceiza A, Mondragon I. Fracture toughness of epoxy resins modified with polyethersulfone: Influence of stoichiometry on the morphology of the mixtures. *Journal of Applied Polymer Science*, 1998, 69(1): 183–191
  41. Yu Y F, Cui J, Chen W J, Li S J. Studies on the phase separation of poly(ether imide) modified tetrafunctional epoxy resin - The effect of curing agent ratio. *Chemical Journal of Chinese Universities-Chinese*, 1998, 19(5): 808–812 (in Chinese)
  42. Reyx D, Campistron I, Caillaud C, Villatte M, Cavedon A. Thermal-reaction between N-phenylmaleimide and 2-allylphenol as a model for the cross-linking reaction in bismaleimide polymerization with diallylbisphenol-a. *Macromolecular chemistry and physics*, 1995, 196(3): 775–785
  43. Mijovic J, Andjelic S. Study of the mechanism and rate of bismaleimide cure by remote in-situ real time fiber optic near-infrared spectroscopy. *Macromolecules*, 1996, 29(1): 239–246

44. Shibahara S, Yamamoto T, Motoyoshiya J, Hayashi S. Curing reactions of bismaleimidodiphenylmethane with mono- or di-functional allylphenols. High resolution solid-state C-13 NMR study. *Polymer Journal*, 1998, 30(5): 410–413
45. Rozenberg A B, Boiko G N, Morgan R J, Shin E E. The cure mechanism of the 4,4'-(*N,N'*-bismaleimide)diphenylmethane-2,2'-diallylbisphenol a system. *Polymer Science Series A*, 2001, 43(4): 386–399
46. Xiong Y, Boey F Y C, Rath K S. Kinetic study of the curing behavior of bismaleimide modified with diallylbisphenol A. *Journal of Applied Polymer Science*, 2003, 90(8): 2229–2240
47. Wisanrakkit G, Gillham J K. The glass-transition temperature ( $T_g$ ) as an index of chemical conversion for a high- $T_g$  amine epoxy system-chemical and diffusion-controlled reaction-kinetics. *Journal of Applied Polymer Science*, 1990, 41(11–12): 2885–2929
48. Zhang X J, Yi X S, Xu Y Z. The effect of chemical structure on the phase separation time/temperature dependencies in some thermoplastics modified thermoset systems. *Acta Polymerica Sinica*, 2007, accepted (in Chinese)